RESEARCH

Evaluation of the behavioral, histopathological, and immunohistochemical effects resulting from ventriculosubcutaneous shunt obstruction in kaolin-induced hydrocephalus in rats

Stephanie Naomi Funo de Souza[1] · Helio Rubens Machado[1] · Luisa da Silva Lopes[2] ·
Pamella da Silva Beggiora Marques[2] · Stephanya Covas da Silva[2] · Maurício Dutra[2] · Davi Casale Aragon[3] ·
Marcelo Volpon Santos[1]

Abstract

Purpose Hydrocephalus is a brain disease prevalent in the pediatric population that presents complex pathophysiology and multiple etiologies. The best treatment is still ventricular shunting. Mechanical obstruction is the most frequent complication, but the resulting pathological effects are still unknown.

Objective Evaluation and comparison of clinical, histopathological, and immunohistochemical aspects in the acute phase of experimental hydrocephalus induced by kaolin, after treatment with adapted shunt, and after shunt obstruction and posterior disobstruction.

Methods Wistar rats aged 7 days were used and divided into 4 groups: control group without kaolin injection ($n = 6$), untreated hydrocephalic group ($n = 5$), hydrocephalic group treated with ventriculosubcutaneous shunt (DVSC) ($n = 7$), and hydrocephalic group treated with shunt, posteriorly obstructed and disobstructed ($n = 5$). The animals were submitted to memory and spatial learning evaluation through the Morris water maze test. The rats were sacrificed at 28 days of age and histological analysis of the brains was performed with luxol fast blue, in addition to immunohistochemical analysis in order to evaluate reactive astrocytosis, inflammation, neuronal labeling, and apoptotic activity.

Results The group with shunt obstruction had worse performance in memory tests. Reactive astrocytosis was more evident in this group, as was the inflammatory response.

Conclusions Obstruction of the shunt results in impaired performance of behavioral tests and causes irreversible histopathological changes when compared to findings in the group with treated hydrocephalus, even after unblocking the system. The developed model is feasible and efficient in simulating the clinical context of shunt dysfunction.

Keywords Ventriculosubcutaneous shunt · Hydrocephalus · Immunohistochemistry · Obstruction

✉ Stephanie Naomi Funo de Souza
naomi.stephanie@gmail.com

1   Division of Pediatric Neurosurgery, Department of Surgery and Anatomy, University Hospital, Ribeirão Preto Medical School, University of São Paulo, Ribeirão Preto 14049-900, Brazil

2   Behavioral Neuropathology and Pediatric Neurosurgery Laboratory, Ribeirão Preto Medical School, University of São Paulo, Ribeirão Preto, SP, Brazil

3   Department of Pediatrics, Ribeirão Preto Medical School, University of São Paulo, Ribeirão Preto, SP, Brazil

Introduction

Hydrocephalus is defined as an increase in the size of the cerebral ventricles secondary to an abnormality in the production, circulation, or reabsorption of cerebrospinal fluid (CSF) [1].

Several pathological processes are involved in altering CSF dynamics and in the genesis of hydrocephalus [2–4], including direct axonal injury, demyelination, cell death, and metabolic and neurotransmitter changes [5].

The diagnosis of hydrocephalus is based on clinical and radiological aspects. Ultrasound (US) is a useful method for diagnosing and monitoring hydrocephalus in children with an open anterior fontanelle [5, 6].

The treatment of hydrocephalus is surgical. Despite the high malfunction rates [2, 7], *shunts* are still the recommended treatment for the vast majority of patients [8], being system obstruction the most common cause of malfunction [7, 9].

Methods

Experimental design

We used a well-established model for experimental hydrocephalus induced by kaolin injection. Forty-three young Wistar rats were randomly selected for the experiment. Twenty-three of them survived. Four groups were formed: control (C; $n = 6$), animals without kaolin injection; non-treated hydrocephalic group (NTH; $n = 5$), animals with confirmed hydrocephalus, no treatment applied; treated hydrocephalic group (TH; $n = 7$), animals with confirmed hydrocephalus treated with a ventriculosubcutaneous shunt (VSCS); and treated hydrocephalic group with shunt obstruction (THOT; $n = 5$), hydrocephalic animals treated with VSCS, which was posteriorly obstructed and then revised. All procedures were undertaken in accordance with the guidelines of the Brazilian College of Animal Experimentation (SBCAL/COBEA) and approved by our institution's ethics committee.

Hydrocephalus induction

Hydrocephalus was induced by intracisternal kaolin injection at 7 days of age. After palpation and identification of the space between the dorsal rim of the foramen magnum and the first cervical vertebra, a suboccipital percutaneous injection was performed, and 0.04 ml of kaolin (aluminum silicate; Sigma, St. Louis, MO) diluted to 20% in distilled water was slowly administered. This technique was previously described by da Silva Lopes et al. [10].

Shunt insertion

Seven days after kaolin injection and confirmation of the ventricular dilatation by cranial ultrasound, animals underwent shunt surgery, as previously described by Santos et al. [11]. After proper material sterilization and anesthesia, a transparent polypropylene catheter was implanted. The proximal (ventricular) portion was inserted through a 2-mm-wide skin incision and 1-mm burr-role anterior to the coronal suture; the distal portion was inserted through a subcutaneous tunnel created over the rat's back until the proximal end of the tail.

Shunt obstruction

In the selected group (THOT), 6 days after shunt insertion and confirmation of the reduction in ventricular dimensions using cranial US, the shunt was occluded by clamping the distal catheter (Fig. 1).

After due preparation (anesthesia, trichotomy, and antisepsis), a skin incision of approximately 5 mm was made over the previously created subcutaneous pocket, until the end of the distal catheter was identified. Using a titanium ligature clip (Weck Horizon, small), the catheter was clamped. After visual confirmation of the interruption of CSF flow, the incision was sutured using Prolene 5-0.

Fig. 1 Scheme showing the catheter used before and after ligation with the clip
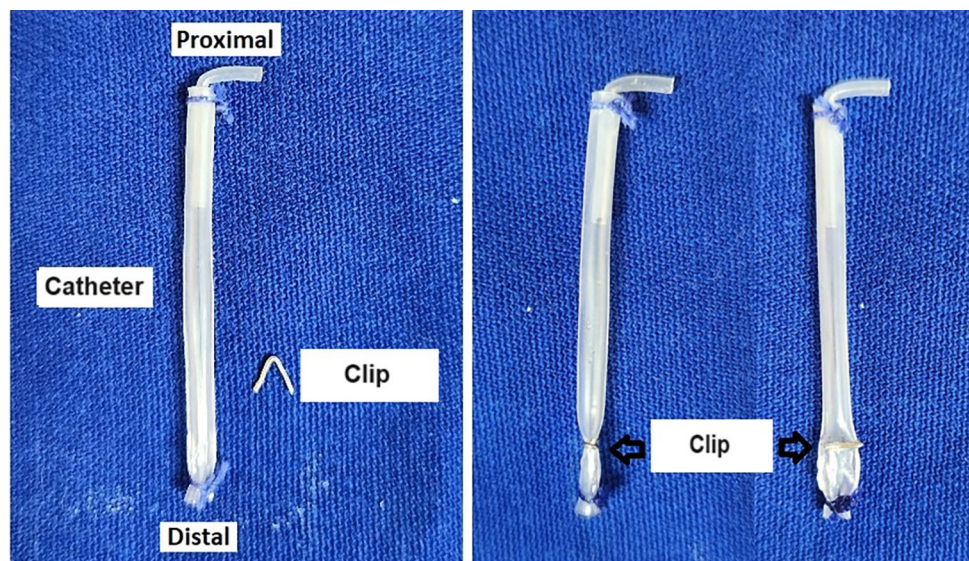
Shunt revision

Three days after the obstruction procedure, recurrence of hydrocephalus was confirmed with cranial US. A new approach was performed, with removal of the ligation clip or section of the distal catheter immediately upstream of the site where the ligation clip was implanted. The anesthetic induction and surgical preparation steps were repeated and the subcutaneous incision was made. The clip was removed or a section on the catheter was made. After visual confirmation of the return of CSF flow, the incision was closed with 5-0 Prolene.

Memory evaluation

The modified Morris water maze test was used to study memory and spatial learning. Initially (adaptation phase), on the 14th day after hydrocephalus induction (P14), the rats had 60 s to swim freely in the pool, without the platform. Next, the platform was introduced into the tank and a luminous point positioned to be used as a reference point. The intention was to allow the rat to locate the camouflaged submerged platform using the iluminated wall as a reference point, rather than randomly finding the platform.

The test was applied again on P15 and P16, in two periods (morning and afternoon). Exceptionally, the animals in the THOT group were subjected to the water maze test at P19 and P20, in order to evaluate memory and spatial learning after a period of hydrocephalus decompensation.

Histological evaluation

Five-micrometer slices of pre-chiasmatic brain sections were obtained on the coronal plane. The luxol fast blue stain was utilized to assess the thickness of the corpus callosum.

Immunohistochemial evaluation

The protocols used in immunohistochemical analysis include blocking endogenous peroxidase with 3% hydrogen peroxide in PBS. Subsequently, blocking is performed with an appropriate 10% serum in PBS for 30 min, in a humid chamber. Then, the sections are incubated overnight at 4 °C with the primary antibody anti-GFAPZ0334 (DAKO, Santa Clara, USA). For anti-COX2 Ab15191, anti-NeuN, and anti-Caspase-3 antibodies, before blocking with endogenous peroxidase, antigen retrieval is performed with heated sodium citrate. After washing the primary antibody, the appropriate secondary antibody (anti-mouse SC-2039—Santa Cruz Biotechnology, TX, USA) diluted 1:300 in BSA is added. Afterwards, they are incubated with the streptavidin conjugate—HRP 405210 (BioLegend, CA, USA) diluted 1:400 in PBS. They are then revealed with DAB (3,3-diaminobenzidine D8001, Merck Millipore, MA, USA).

Through the immunohistochemical study using glial fibrillary acidic protein (GFAP), a quantitative and qualitative analysis of the astrocytic reaction was carried out by counting reactive astrocytes in an area of 1 mm^2 (cell density) and grading the marking intensity (score), respectively. The search for reactive astrocytes was carried out in four regions: corpus callosum (CC), germinal matrix (MG), cerebral cortex dorsal to the corpus callosum (CTX_F), and hippocampus (CA1, CA2, CA3, and GD).

Analysis of Caspase-3, a cytoplasmic protein, was used to evaluate apoptosis in brain tissue. A scan was made along the entire length of the CTX_F and from the dorsal cortex to the hippocampus (CTX_D).

Immunohistochemistry for cyclooxygenase-2 (COX-2) was performed to assess neuroinflammation. The regions of CTX_F, CTX_D, CC, and MG were analyzed, as were the hippocampal subareas (CA1, CA2, CA3, and GD). Immunostained cells were counted and the labeling density was calculated (positive cells / total cells × 100).

To determine whether hydrocephalus and its respective studied treatments alter/preserve the total number and density of neurons, we performed immunohistochemical analysis for NeuN (neuronal nuclei). The regions of the CTX_F, the hippocampal subareas (CA1, CA2, CA3, and GD), and the CTX_H were analyzed. Cell density (total number of neurons / area) and labeling percentage (positive cells / total cells × 100) were calculated.

Statistical analysis

Data were presented as means (or median) and standard deviation. For normality testing, the Kolmogorov-Smirnov test was used. For parametric data, analysis of variance (ANOVA) was used, followed by Tukey's post-test, when indicated. For non-parametric data, the test used was the Kruskall-Wallis, followed by the Dunn post-test. Statistical differences were considered when $p < 0.05$. The GraphPad Prism 9.0 (GraphPad Software In., San Diego, CA, USA) and SAS 9.4 programs were used.

Results

Memory assessment

The THOT group, during its first evaluation, presented the longest arrival time among the other animals studied, with a significant difference in all periods compared to all other groups.

Table 1 Comparison between all different groups, in the same period. For the THOT group, the first evaluation was considered

Comparison	Mean difference	p value	IL	SL
(C-NTH) M1	−8.62	0.07	−21.24	3.99
(C-TH) M1	−9.14	0.03	−19.38	1.13
(C-THOT1) M1	−33.92	<0.01	−47.48	20.37
(NTH-TH) M1	−0.50	0.46	−13.50	12.51
(NTH-THOT1) M1	−23.55	0.01	−42.71	4.38
(TH-THOT1) M1	−24.80	<0.01	−38.56	11.04
(C-NTH) T1	−4.91	0.24	−20.12	10.29
(C-TH) T1	−1.49	0.38	−12.44	9.46
(C-THOT1) T1	−19.47	0.04	−42.40	3.47
(NTH-TH) T1	3.42	0.23	−10.97	17.82
(NTH-THOT1) T1	−14.55	0.10	−38.98	9.88
(TH-THOT1) T1	−17.98	0.07	−45.16	9.21
(C-NTH) M2	−1.17	0.24	−4.86	2.51
(C-TH) M2	−10.16	0.03	−21.77	1.45
(C-THOT1) M2	−22.52	0.02	−42.36	2.69
(NTH-TH) M2	−8.98	0.05	−22.17	4.20
(NTH-THOT1) M2	−21.35	0.02	−44.57	1.87
(TH-THOT1) M2	−12.36	0.07	−30.11	−5.38
(C-NTH) T2	−7.22	0.05	−16.55	2.10
(C-TH) T2	−9.20	<0.01	−13.93	4.46
(C-THOT1) T2	−26.52	<0.01	−40.06	12.99
(NTH-TH) T2	−1.97	0.29	−9.67	5.73
(NTH-THOT1) T2	−19.30	<0.01	−32.83	5.77
(TH-THOT1) T2	−17.32	<0.01	−27.28	7.24

C control group, *NTH* non-treated hydrocephalic group, *TH* treated hydrocephalic group, *THOT1* treated hydrocephalic group, with shunt obstruction, first evaluation

After shunt revision, the animals of the THOT group were subjected to a new evaluation. A reduction in arrival

Table 2 Comparison between different groups, in the same period. For the THOT group, the second evaluation was considered

Comparison	Mean difference	p value	IL	SL
(C-THOT2) M1	−22.82	<0.01	−37.29	8.35
(NTH-THOT2) M1	−14.20	0.05	−32.27	3.86
(TH-THOT2) M1	−13.07	0.03	−28.20	0.80
(C-THOT2) T1	−7.41	0.18	−24.89	10.05
(NTH-THOT2) T1	−2.50	0.37	−20.26	15.28
(TH-THOT2) T1	−5.93	0.16	−18.69	6.83
(C-THOT2) M2	−5.62	0.15	−18.93	7.68
(NTH-THOT2) M2	−4.45	0.20	−16.02	7.12
(TH-THOT2) M2	4.53	0.25	−10.28	19.35
(C-THOT2) T2	−6.57	0.04	−14.83	1.68
(NTH-THOT2) T2	0.65	0.44	−9.53	10.83
(TH-THOT2) T2	2.62	0.21	−4.52	9.76

C control group, *NTH* non-treated hydrocephalic group, *TH* treated hydrocephalic group, *THOT2* treated hydrocephalic group, with shunt obstruction, second evaluation

Table 3 Comparison between the same group, in different periods, different evaluations

Comparison	p value	IL	SL
(M1-T1) THOT-1	0.16	−13.97	36.97
(M1-M2) THOT-1	0.06	−4.87	36.68
(M1-T2) THOT-1	0.03	−1.55	32.38
(T1-M2) THOT-1	0.36	−23.08	31.89
(T1-T2) THOT-1	0.36	−20.82	28.62
(M2-T2)THOT-1	0.47	−20.35	19.35
(M1-T1) THOT-2	0.09	−7.56	32.45
(M1-M2) THOT-2	0.01	3.95	39.44
(M1-T2) THOT-2	<0.01	8.75	39.75
(T1-M2) THOT-2	0.13	−8.77	27.27
(T1-T2) THOT-2	0.06	−4.02	27.61
(M2-T2) THOT-2	0.32	−10.30	15.40

THOT1 treated hydrocephalic group, with shunt obstruction, first evaluation, *THOT2* treated hydrocephalic group, with shunt obstruction, second evaluation

time compared to the first assessment was observed in all periods considered.

Despite the improvement in the performance of the THOT group between the first and second assessments, there was still a difference between the arrival times of this group in relation to all other groups.

The results are shown in Tables 1, 2, 3, and 4.

Histological results

Utilizing the luxol fast blue stain, there was a difference in the thickness of the corpus callosum between the groups, confirmed by statistical analysis ($p < 0.01$). The control group showed the greatest thickness compared to the others (Table 5).

Immunohistochemical results

Qualitative assessment of the corpus callosum showed that the THOT group presented a more intense astrocytic reaction compared to the other groups, with a large number of astrocytes per area, intensely marked, with coarse

Table 4 Comparison between the same group, in the same period, different evaluations

Comparison	Mean difference	p value	IL	SL
(THOT1-THOT2) M1	11.10	0.1	−7.84	30.01
(THOT1-THOT2) T1	12.05	0.16	−14.24	38.34
(THOT1-THOT2) M2	16.90	0.04	−2.82	36.62
(THOT1-THOT2) T2	19.95	<0.01	6.91	32.99

THOT1 treated hydrocephalic group, with shunt obstruction, first evaluation, *THOT2* treated hydrocephalic group, with shunt obstruction, second evaluation

Table 5 Difference in the thickness of the corpus callosum between groups

Groups	Mean thickness (µm)	SD
Control	354.81	33.06
NTH	215.76	101.94
TH	191.43	98.68
THOT	194.75	59.44

and irregular extensions, although not statiscally confirmed ($p = 0.22$ and $p = 0.20$ for density and intensity of astrocytic reaction, respectively).

In the germinal matrix, both surgical groups showed a greater number and higher intensity of marking ($p = 0.03$), revealing an intense astrocytic reaction.

In the CTX_F, the THOT group also showed greater density ($p < 0.01$ compared to the control group) and intensity of the astrocytic reaction compared to the other groups ($p = 0.22$).

The THOT group showed a large number of reactive astrocytes in the CA1, CA2, and dentate gyrus subareas, in contrast to the cell density demonstrated in the control group. The intensity of labeling varied between groups in different regions. Statistical analysis found no difference between the previously described findings.

Analysis of caspase-3 immunostaining showed contrasting changes between the regions. In the CTX_F, a greater density of apoptotic cells was noted in the THOT group. In the cerebral cortex CTX_D, in turn, a greater number of cells undergoing apoptosis were noted in the TH group. None of these findings was statistically relevant ($p = 0.09$ and $p = 0.43$, respectively).

The qualitative evaluation of COX-2 immunostaining demonstrated a large percentage of labeled cells in the THOT group compared to the other groups, both in the corpus callosum ($p = 0.24$) and in the germinal matrix ($p = 0.02$).

In the cerebral cortex, the THOT group showed the greatest variation, demonstrating a high percentage of labeled cells in the CTX_F, but a low percentage in the CTX_D. These findings had no statistical relevance ($p = 0.38$ and $p = 0.07$).

In the analysis of the hippocampal subareas, the NTH group presented the highest percentage of cells with immunostaining for COX-2 in all regions analyzed. The greatest discrepancy in labeling occurred in CA3 and the dentate gyrus, with the THOT group showing a much lower percentage of labeled cells compared to the other groups. The findings, however, were not statistically significant.

The percentage of cells immunostained for Neu-N and the density of neuronal cells were analyzed. The qualitative evaluation of the sheets of the CTX_F showed a greater number of neuronal cells in the THOT group ($p = 0.03$). When analyzing the percentages of marked cells, the differences were less evident ($p = 0.45$).

In the CTX_D, cell density was higher in the THOT group ($p = 0.02$). The percentages of cells with immunostaining varied in this region ($p = 0.07$).

In the hippocampal subareas, the density of neuronal cells was higher in the THOT group. confirmed only in CA3 ($p = 0.02$). In the analysis of the percentage of immunostained cells, there was also statistical confirmation of the difference between the groups in CA3 ($p = 0.03$) between the THOT and NTH groups ($p = 0.01$), and control and NTH groups ($p < 0.01$).

Discussion

The main objective of this study was to analyze the clinical and histopathological changes caused by the recurrence of hydrocephalus secondary to shunt dysfunction.

The Morris water maze test is well established in the literature due to its easy application, reliability, applicability, and evidence of its validity as an assessment of spatial memory [12].

The test was performed on the P14 and P15 in all groups. The THOT group, exceptionally, was evaluated again on the P19 and P20.

Despite memory impairment, hydrocephalic animals still have the ability to learn. In the present study, when considering the performances within the same group, the THOT group showed improvements in the first and second assessments.

In the comparative analysis between groups, the THOT group, during its first evaluation, presented the longest arrival time among the other animals studied. After unblocking the system, a reduction in arrival time was observed compared to the first assessment in all periods considered. Despite the improvement in the performance between the first and second assessments, there was still a significant difference between the arrival times of this group in relation to others.

These findings show that despite the improvement in performance after shunt revision, the impairment in spatial memory was irreversible during the period studied: the performance of the THOT group was inferior despite the treatment implemented and despite the greater chronological age of this group at the time of comparison (animals in the THOT group were 26 and 27 days old in their second evaluation).

Through histological study with luxol fast blue, the control group had the highest average thickness of the corpus callosum compared to the other groups. Furthermore, the untreated hydrocephalic group had a smaller thickness of the corpus callosum compared to the groups undergoing treatment, with or without obstruction. These findings demonstrate that surgical treatment, if instituted in a timely manner, is capable of partially reversing the involvement of the periventricular white matter.

Through an immunohistochemical study using GFAP, a quantitative and qualitative analysis of the astrocytic reaction was carried out.

In the study of the corpus callosum sheets, the THOT group showed a more intense astrocytic reaction compared to the other groups: in addition to the greater astrocytic density, the cells were intensely marked, with coarse and irregular extensions. Astrocytic density and reaction intensity were higher in the surgical groups, even compared to the untreated hydrocephalic group. The inflammatory reaction in response to surgical trauma and the presence of a ventricular catheter can be considered as a possible cause for this finding. Furthermore, it is known that the reconstitution of the periventricular white matter also occurs at the expense of astrocytic proliferation, resulting in an increase in the immunoreaction for GFAP. In the present study, an intense astrocytic reaction was evident in the THOT group, and this discrepancy could be explained both by the recurrence of hydrocephalus and by multiple surgical approaches.

The evaluation of the germinal matrix slides showed differences between all groups. The slides from the surgical groups demonstrated a greater number and greater intensity of marking compared to the control and NTH groups. The THOT group not only demonstrated a greater intensity of the astrocyte reaction, but also a tendency towards a greater number of reactive astrocytes.

In the present study, it was noted that the astrocytic reaction in the CTX_F was less evident in this region when compared to the periventricular regions. However, as previously described, the groups with untreated hydrocephalus and the groups undergoing surgical treatment, especially the THOT group, demonstrated a more intense astrocytic reaction than the animals in the control group.

The same pattern can be observed in the CA1 and CA2 subareas of the hippocampus: the groups undergoing surgical treatment demonstrated a higher astrocytic density than the others; the intensity of the reaction was varied. In the dentate gyrus, a greater number of reactive astrocytes were evident in the groups with untreated hydrocephalus and obstructed shunt compared to the others.

A possible explanation for the presence of the intense astrocytic reaction in the group that had the shunt obstructed would be the cumulative effect of the lesions caused by hydrocephalus before treatment and after the catheter was obstructed. Furthermore, considering the possible beneficial effect of the astrocytic reaction on the reconstitution of brain tissue (Aoyama et al. 2006), intense immunostaining with GFAP may also be associated with the treatment of hydrocephalus. In contrast to the treated hydrocephalic group, in which euthanasia was performed 21 days after the procedure, euthanasia in the THOT was performed only 3 days after the last procedure, thus reducing the time available for reduction in the astrocytic response in this group.

When analyzing caspase-3 immunostaining, the findings were contrasting between the different regions, as previously stated. Caspases are involved in the process of programmed cell death essential for brain development, in addition to being effectors in the destruction of aberrant or dysfunctional synapses and axonal connections [13]. Furthermore, it has been demonstrated they are also inducers of cellular apoptosis in response to traumatic and ischemic stimuli [14]. Despite the mechanism that led to the initiation of the apoptosis process, cells in the process of cell death can only be visualized for a short period of time before their disappearance [15].

These factors may have influenced the differences found between the two regions analyzed. Firstly, it was not possible to differentiate whether the cellular immunostaining by caspase occurred in response to the damage induced by hydrocephalus or whether it corresponded to programmed cell death that would occur during brain development. Secondly, the evaluation was carried out on the 28th day after birth in all animals from all groups: the analysis of the slides in a single period does not allow us to conclusively determine in which groups and in which regions there was the highest rate of cell death due to apoptosis.

Cyclooxygenase-2 is an enzyme that catalyzes the transformation of arachidonic acid into several bioactive substances, known as prostaglandins [16, 17]. Increased expression of COX-2 has been associated with neurotoxicity in acute insults to the nervous system, such as hypoxia, ischemia, and seizures [16]. However, strong evidence suggests that COX-2 also exerts essential physiological neuronal functions, being constitutively expressed in some organs such as kidneys, testicles, and brain.

In rat brains, physiological expression of COX-2 occurs in neuronal cells; in contrast, in the inflammatory response, COX-2 expression occurs mainly in astrocytes and microglia [17]. It is possible that COX-2 expression in the hippocampus plays an important role in acquisition and processing of spatial memory [18].

Qualitative evaluation demonstrated a large percentage of labeled cells in the THOT group compared to the other groups, both in the corpus callosum and in the germinal matrix. We can infer from these results that the inflammatory response in these regions was greater in this group.

In the cerebral cortex, the THOT group showed great variation in the percentage of COX-2 immunoexpression, demonstrating a high percentage of labeled cells in the CTX_F, but a low percentage in the CTX_D.

In the analysis of the hippocampal subareas, the THOT group showed a much lower percentage of labeled cells in CA3 and dentate gyrus. The lower percentage of marked

cells in the THOT group may justify the worse performance of these animals in the Morris water maze test.

In the other regions, the percentage of cells with immunostaining for COX-2 was very similar, which may reflect a lower degree of damage in these areas of the hippocampus.

To evaluate the effects of hydrocephalus on the neuronal cell population, Neu-N immunostaining was used. Evaluation of the cerebral cortex showed a greater number of neuronal cells in the THOT group in relation to the other groups, both in CTX_F and in CTX_D. However, when analyzing the percentages of labeled cells, the differences were less evident. The increase in the population of neuronal cells may reflect an attempt to increase cell proliferation in response to the insults caused by both hydrocephalus and the established treatments.

In the hippocampal subareas, the density of neuronal cells was also higher in the THOT group. Despite the apparent lesser severity of the injury caused by hydrocephalus in the hippocampal region, the same mechanisms that justify the greater cell density in the THOT group can be applied to this region.

Conclusions

This study aimed to evaluate possible behavioral and histopathological changes resulting from the recurrence of hydrocephalus due to shunt obstruction, a situation prevalent in clinical practice. Although most of the findings could not be confirmed by statistical analysis, probably due to a small sampling, a new technique was developed that simulates the main cause of shunt malfunction. To date, it is an unprecedented study in the medical literature. Based on the model developed in this work, new study designs can be implemented, aiming to minimize the biases found during the course of this experiment. The model proved to be feasible and efficient in simulating shunt obstruction.

Declarations

Ethics approval All procedures were undertaken in accordance with the guidelines of the Brazilian College of Animal Experimentation (SBCAL/COBEA) and approved by our institution's ethics committee.

Conflict of interest The authors declare that they have no conflict of interest.

References

1. Williams MA, McAllister JP, Walker ML et al (2007) Priorities for hydrocephalus research: report from a National Institutes of Health-sponsored workshop. J Neurosurg 107:345–357

2. McAllister JP 2nd (2012) Pathophysiology of congenital and neonatal hydrocephalus. Semin Fetal Neonatal Med 17:285–294

3. Nagra G, Del Bigio MR (2018) Pathology of pediatric hydrocephalus. Pediatric hydrocephalus. Springer International Publishing, Cham, pp 1–25

4. Mcallister JP, Eskandari R, Limbrick DD (2016) Experimental hydrocephalus. In: Youmans and Winn neurological surgery. Elsevier Health Sciences

5. Jamil O, Kestle JRW (2016) Hydrocephalus in children: etiology and overall management. In: Youmans neurological surgery. Elsevier Health Sciences

6. Dinçer A, Özek MM (2011) Radiologic evaluation of pediatric hydrocephalus. Childs Nerv Syst 27:1543–1562

7. Hanak BW, Bonow RH, Harris CA, Browd SR (2017) Cerebrospinal fluid shunting complications in children. Pediatr Neurosurg 52:381–400

8. Del Bigio MR (2001) Future directions for therapy of childhood hydrocephalus: a view from the laboratory. Pediatr Neurosurg 34:172–181

9. Paff M, Alexandru-Abrams D, Muhonen M, Loudon W (2018) Ventriculoperitoneal shunt complications: a review. Interdiscip Neurosurg 13:66–70

10. da Silva Lopes L, Slobodian I, Del Bigio MR (2009) Characterization of juvenile and young adult mice following induction of hydrocephalus with kaolin. Exp Neurol 219:187–196

11. Santos MV, Garcia CAB, Jardini EO et al (2016) Ventricular-subcutaneous shunt for the treatment of experimental hydrocephalus in young rats: technical note. Childs Nerv Syst 32:1507–1511

12. Vorhees CV, Williams MT (2006) Morris water maze: procedures for assessing spatial and related forms of learning and memory. Nat Protoc 1:848–858

13. Hyman BT, Yuan J (2012) Apoptotic and non-apoptotic roles of caspases in neuronal physiology and pathophysiology. Nat Rev Neurosci 13:395–406

14. Yakovlev AG, Faden AI (2001) Caspase-dependent apoptotic pathways in CNS injury. Mol Neurobiol 24:131–144

15. Thomaidou D, Mione MC, Cavanagh JF, Parnavelas JG (1997) Apoptosis and its relation to the cell cycle in the developing cerebral cortex. J Neurosci 17:1075–1085

16. Minghetti L (2004) Cyclooxygenase-2 (COX-2) in inflammatory and degenerative brain diseases. J Neuropathol Exp Neurol 63:901–910

17. López DE, Ballaz SJ (2020) The role of brain cyclooxygenase-2 (Cox-2) beyond neuroinflammation: neuronal homeostasis in memory and anxiety. Mol Neurobiol 57:5167–5176

18. Kaufmann WE, Worley PF, Pegg J et al (1996) COX-2, a synaptically induced enzyme, is expressed by excitatory neurons at postsynaptic sites in rat cerebral cortex. Proc Natl Acad Sci USA 93:2317–2321